

Comprehensive relationship analysis of the Long Non-Coding RNAs (lncRNAs) and the target mRNAs in Response to the infection of *Edwardsiella anguillarum* in European eel (*Anguilla Anguilla*) inoculated with Freund's adjuvant

Liqun Wu

Jimei University

Zhijie Yin

Jimei University /Engineering Research Center of the Modern Industry Technology for Eel. Ministry of Education of PRC

Zhijin Zheng

Jimei University /Engineering Research Center of the Modern Industry Technology for Eel. Ministry of Education of PRC

Yijun Tang

University of Wisconsin Oshkosh

Songlin Guo (✉ gsl@jmu.edu.cn)

Jimei University /Engineering Research Center of the Modern Industry Technology for Eel. Ministry of Education of PRC

Research Article

Keywords: lncRNA, *Edwardsiella anguillarum*, *Anguilla anguilla*, Freund's adjuvant, Anti-infection

Posted Date: May 17th, 2022

DOI: <https://doi.org/10.21203/rs.3.rs-1649271/v1>

License:   This work is licensed under a Creative Commons Attribution 4.0 International License. [Read Full License](#)

Abstract

Freund's complete (FCA) and incomplete adjuvants (FIA), generally applied in subunit fishery vaccine, have not been explored on the molecular mechanism of the nonspecific immune enhancement. As long noncoding RNAs (lncRNAs) play vital regulating roles in various biological activities, in this study, we examined the genome-wide expression of transcripts in the liver of European eel (*Anguilla anguilla*, *Aa*) inoculated with FCA and FIA (FCIA) to elucidate the regulators of lncRNAs in the process of *Edwardsiella anguillarum* (*Ea*) infection and *Aa* anti-*Ea* infection using strand specific RNA-seq. After eels were challenged by *Ea* at 28 d post the first inoculation (dpi), compared to the control uninfected eels (Li group), the control infected eels (Con_Li group) showed severe bleeding, hepatocyte atrophy and thrombi formed in the hepatic vessels of the liver, although eels inoculated with FCIA (FCIA_Li group) also formed slight thrombi in the hepatic vessels. Compared to the FCIA_Li group, there was about 10 times colony forming unit (cfu) in the Con_Li group per 100 µg liver tissue, and the relative percent survival (RPS) of eels was 50% in FCIA_Li vs Con_Li. Using high-throughput transcriptomics, differential expressed genes (DEGs) and transcripts were identified and the results were verified using fluorescence real-time polymerase chain reaction (qRT-PCR). Interactions between the differential expressed lncRNAs (DE-lncRNAs) and the target DEGs were explored using Cytoscape according to their co-expression and co-location relationship. We found 13499 lncRNAs (10176 annotated and 3423 novel lncRNAs) between 3 comparisons of Con_Li vs Li, FCIA_Li vs Li and FCIA_Li vs Con_Li, of which 111, 110 and 129 DE-lncRNAs were ascertained. Gene ontology (GO) and Kyoto Encyclopedia of Genes and Genomes (KEGG) analysis of DEGs targeted by DE-lncRNAs revealed these DEGs mainly involved in single-organism cellular process in BP, membrane in CC and binding in MF, and KEGG pathways showed that the target DEGs in co-expression and co-location enriched in cell adhesion molecules. Finally, 118 DE-lncRNAs target 1161 DEGs were involved in an interaction network of 8474 co-expression and 333 co-location related links, of which 16 DE-lncRNAs play vital roles in anti-*Ea* infection. Taken together, the interaction networks revealed that DE-lncRNAs underlies the process of *Ea* infection and *Aa* anti-*Ea* infection.

1. Introduction

Edwardsiella anguillarum (*Ea*) is a common bacterial pathogen mainly infected cultivated eel (Reichley et al., 2017; Guo et al., 2019). At present, the research on *Edwardsiella* focuses on finding a protein with universal antigenicity to different serotypes, and the results showed that bivalent expressed outer membrane protein (OMP) generally had good immunogenicity (Guo et al., 2013; Zhang et al., 2016). The expressed outer membrane protein OmpS₂ showed good immunogenicity and can be applied as a kit for *E. tarda* detection (Kumar et al., 2007). OmpA of *Ea* was also evaluated as an antigen with good immunogenicity in Japanese Flounder *Paralichthys olivaceus* (Tang et al., 2010). The above-mentioned OMP vaccine were emulsified with Freund's complete (FCA) or incomplete adjuvant (FIA) to enhance the protective effect, and the control adjuvant group designed by researchers also produced protective effect after the challenge of different bacterial pathogens (Duan et al., 2019). Additionally, examination of the transcription profile of immune-related genes showed that vaccination with FIA adjuvant OMP (*E. tarda* 49) induced the expression of a broader spectrum of genes that are likely to be involved in humoral and innate cellular immunity (Jiao et al., 2010). The relative percentage survival (RPS) for FIA-adjuvanted vaccine (77.8%) were higher than the vaccine without adjuvant (40.7%) after FIA incorporated with inactivated *Streptococcus agalactiae* for Nile

tilapia fingerlings (Ramos-Espinoza et al., 2020) as well as the FCA adjuvant induced non-specific immunity in cultured fish and increased 5.3 to 450 times of LD₅₀ on *Aeromonas salmonicida*, *A. hydrophila* and *Vibrio ordalii* challenge in coho salmon *Oncorhynchus kisutch*, respectively (Olivier et al., 1985). However, there is no study focused on FCA and FIA inoculated sequentially and no molecular mechanism of the non-specific immune protection activated by the FCA and FIA (He et al., 2020). Recently, it was found that the *Ea* mainly invaded the liver of European eels post 48 h of the infection (Zhai et al., 2021), and two times of immunization of OmpA emulsified with FCA and FIA respectively showed long non coding RNA (lncRNA) played crucial role in regulating many immune-related proteins (He et al., 2021). lncRNA, a kind of RNA molecule with a length of more than 200 nt, have been ignored as useless transcripts for a long time (Yousefi et al., 2020). In recent years, more and more studies have proved that lncRNA is widely existed in eukaryotes, and plays an important role in all kinds of animals (Robinson et al., 2020; Valenzuela-Muñoz et al., 2021; Aciole Barbosa et al., 2022). In fish, integrated analysis of lncRNA and mRNA expression showed anti-infection regulation of lncRNAs post the infection of *E. tarda* and *Ea* (Xiu et al., 2021; Zhao et al., 2021; He et al., 2021). However, there is no study on the anti-infection effect of lncRNAs activated by the bacterial pathogen after animals inoculated with adjuvant. Since the adjuvants of FCA and FIA have been widely used in fishery vaccine, it is of great significance to explore its molecular immune mechanism. The aim of this study is to explore the relationship between the differential expressed lncRNAs (DE-lncRNAs) and the target DE-mRNAs activated by the *Ea* infection pre and post the inoculation of FCA and FIA in European eels (*Anguilla anguilla*, *Aa*). Results of this study will reveal the molecular response of Freund's adjuvant to bacterial infection in fishery vaccine.

2. Materials And Methods

2.1 Bacterial Strain and Fish

The pathogen of *Edwardsiella anguillarum* (*Ea* B79) was isolated from the liver of diseased eels and identified by the Biolog Gene $\text{\textcircled{R}}$ system and sequencing analysis of OmpA genes (Duan et al., 2019). One hundred and twenty European eels (40 \pm 10g) were obtained from QingLiu county, Fujian province and randomly assigned into 3 groups. Eels were placed in 500-liter tanks under controlled conditions with aerated fresh water and kept at 28 °C for 14 d prior to the inoculation. During the experiment, eels were fed commercial pellets (Tianma Feed Co., Ltd, Fuqing, China) once a day. Feces of fish and feed remnants were removed after 2 to 3 h of feeding.

2.2 Inoculation, Experimental Challenge and Liver Sampling

Culture of *Ea* was prepared using Tryptone soya broth (TSB), and the bacterial cells were concentrated to 3.0 \times 10⁷ cfu ml⁻¹ (Xiao et al., 2021). The Freund's complete (FCA) and incomplete adjuvants (FIA) was mixed with equal volume of PBS (0.01M, pH = 7.4). After the injection of 0.2 ml PBS per fish at 0 d and 14 d, 80 European eels were divided equal into 2 groups of PBS injected (Li group) and *Ea* infected (Con_Li group) fish which received 0.2 ml/fish of PBS and 3.0 \times 10⁷ cfu/ml *Ea* respectively at 28 day post the first injection (dpi). Simultaneously, 40 eels were inoculated with 0.2 ml/fish of FCA and FIA at 0 d and 14 d respectively (FCIA_Li group), and all eels were challenged by the *Ea* at 28 d post the FCA inoculation. At 24 and 48 h post the

challenge (hpc) respectively, 3 eels in each group were anesthetized by immersion in water containing 100 ppm Eugenol for 10 min and then all livers were collected. The remaining eels in two infected groups were used to ascertain the relative percent of survival (RPS) in 14 d post the challenge (dpc) as the method of He et al. (2020).

2.3 Bacterial Load, Pathological Observation and Total RNA Extraction

After 18 livers collected in the method of 2.2 were carefully examined, 9 livers (3 livers/group) collected at 24 hpc were used to detect the colony quantity of bacterial load in the liver (cfu/mg). Another 9 livers (3 livers/group) collected at 48 hpc were cut into 3 pieces. One piece of each liver was placed in 10% medium formalin and processed for paraffin embedding as He et al. (2021), and 4- μ m sections were cut from each liver and stained with hematoxylin and eosin (H & E). Images of each H & E-stained liver were acquired by Leica Scan 500 slide scanner equipped with 20 \times lens. Another 2 pieces of each liver were collected for bacterial plate colony count and total RNA extraction respectively as the method of Zhai et al. (2021).

2.4 Transcriptome of Strand Specific RNA Sequencing

To obtain the RNA-seq data from 9 liver samples, the flow process of sample detection, database construction and sequencing in Novogene (Beijing, China) is as follows: total RNA sample detection; rRNA removal; synthesis of double stranded cDNA; cDNA purification; ending cDNA repair and adding A-tail and adaptor; fragment selection, degradation of the second chain of cDNA, PCR enrichment, library quality inspection and illumine 3000 sequencing. To detect the mapping rates, clean reads were aligned with the genome of *A. anguilla* by the software of Biwtie2

(https://www.ncbi.nlm.nih.gov/assembly/GCF_013347855.1).

2.5 Genome Alignment and Quantification of gene and transcripts

The expression of each gene was quantified by RSEM software. The proportions of reads in exons, introns and intergenic regions according to the comparison results were calculated. The reads in the intron region may come from the precursor mRNA or the introns retained by alternative splicing events, and reads in the intergenic region may come from lncRNA (Alessandra et al., 2017). The software of Stringtie has specific parameters for different libraries, which can accurately splice transcripts and achieve transcriptional quantification (Pertea et al., 2015). In this study, Stringtie was used to splice the reads which mapped on the genome into transcripts and quantify it (Ghosh and Chan, 2016). All transcripts were merged by the Cuffmerge software to remove transcripts length less than 200 nt or with uncertain chain direction. The remaining transcripts were compared with known databases and the gene function annotation of known transcripts were obtained according to the annotation file of *A. anguilla* (.gff). For unknown transcripts, CPC2, Pfam and CNCI were used to predict the coding potential. If the transcripts had no coding potential by these software, the candidate transcripts are predicted as novel_lncRNAs (XR_), and if the candidate transcripts are found to have coding potential, it will be predicted as novel_mRNAs (Harrow et al., 2012).

2.6 Analysis of Differentially Expressed lncRNA

In this study, up or down functional Gene, mRNA and lncRNA were classified based on Fragments Per Kilobase per Million (FPKM). When compared 9 samples, the total clusters of DEGs or DE-transcripts found by EdgeR with $p_{adj} < 0.05$ were showed by heat and volcano map (Varet et al., 2016). Using the mainstream hierarchical clustering method, the $\log_{10}(fpkm + 1)$ value was transformed and clustered. The clustering results are represented by Heatmap of Gene, mRNA and lncRNA. Venn and volcano map, which directly showed the cross and overall distribution genes with significant difference expression between 3 groups, were constructed to find the key lncRNAs in the process of anti-infection. Functional analysis of gene ontology (GO) and Kyoto Encyclopedia of genes and genomes (KEGG) focuses on DEGs with biological functions. Goseq (Young et al., 2010) based on Wallenius non central hyper geometric distribution mathematical model was used to analyze top 20 significant GO enrichments ($qvalue < 0.05$) of molecular function (MF), cellular component (CC) and biological process (BP) in DEGs. KOBAS software (version 2.0) was used to analyze the KEGG pathway enrichment of DE-lncRNAs ($p_{adj} < 0.05$) target genes based on hyper geometric test.

2.7 RT-PCR Validation

To validate the results of gene expression obtained from RNA-seq, cDNA samples of 23 immune related genes were selected and verified by qRT-PCR between FCIA_Li and Con_Li. The analysis was performed using the RealUniversal Color PreMix (SYBR Green) (Tiangen, Beijing, China) on a LightCycler® 480 (Roche, USA). The first-strand cDNA of DEGs of *Aa* was first synthesized as templates for qRT-PCR with specific primers, and β -actin was used as an internal control (Table 1). Preparation of samples and the amplification procedure were referenced as He et al. (2020). Data were analyzed using the Excel and relative expression of DEGs was determined using the $2^{-\Delta\Delta Ct}$ algorithm, and then compare to the results of RNA_seq.

Table 1
Primers used for real-time PCR of 23 genes of European eels (*A. anguilla*)

Gene ID	Gene name	Gene description	Primers for qRT-PCR(5'-3')
/	/	β -actin (housekeeping)	f-aatccacgagaccaccttcaa; r-gttggcgtacaggctccttacg
118231227	slc7a11	solute carrier family 7 member 11	f-aatccacgagaccaccttcaa; r-gttggcgtacaggctccttacg
118217616	acss1	acyl-CoA synthetase short chain family member 1	f-gcctcttcacatccaagctg; r-tgtgcaagtcctctggat
118232520	LOC118232520	E3 ubiquitin-protein ligase HERC3	f-taccttccgcaggctatctg; r-cttgggttcacgittgggt
118230117	LOC118230117	apolipoprotein A-I-like	f-tgtccaaacgcagactctct; r-gctggagctggtgaatgatg
118226107	serpinc1	serpin peptidase inhibitor, clade C (antithrombin), member 1	f-tatctccactgcctttgcca; r-ttagccaacatcagggtccgt
118225677	LOC118225677	flavin-containing monooxygenase 5-like	f-ctctgcttagcgcacacat; r-gaagacgctcatgtgcagt
118235607	c1qa	complement component 1, q subcomponent, A chain	f-aacctgtgtctggctctgaa; r-gtcatgtggtggccagttt
118223465	LOC118223465	asialoglycoprotein receptor 1-like, transcript variant X1	f-gttctgagcctccagggaa; r-attctgtagcagcactgggt
118231169	c4b	complement 4B (Chido blood group)	f-tcctttgccagggtgaacaga; r-acaccagcagcaaatatggg
118212951	LOC118212951	lysozyme C-like	f-ccattcctcctcgtaggctt; r-cccattgggatctctgacca
118220208	LOC118220208	guanylate-binding protein 1-like	f-ccgtcatcatgoggatcttc; r-ggaatccaactccgttctgc
118235666	LOC118235666	alpha-2-macroglobulin-like	f-acctgtggtgctggaaacta; r-cctggctggagacagtgtta
118221855	LOC118221855	cell death-inducing p53-target protein 1 homolog, transcript variant X1	f-agctgccctacctgtaagtg; r-acgtcaccaaccagatgat
118231298	LOC118231298	H-2 class II histocompatibility antigen, A-U alpha chain-like, transcript variant X1	f-ttgttgtgcttgccctcaca; r-tgcctgtgattctcttgggt
118234441	LOC118234441	H-2 class I histocompatibility antigen, Q8 alpha chain-like, transcript variant X1	f-gagcaaaggagactcaggt; r-tgacgtcttcagagccagt
118226566	irf2bpl	interferon regulatory factor 2 binding protein-like	f-agactgtaacgtgccttgga; r-acaagaggcaaggagtcgaa
118214202	tlr22	toll-like receptor 22	f-cattccagagctcaccatgc; r-tgcttcacctgtagggactg

Gene ID	Gene name	Gene description	Primers for qRT-PCR(5'-3')
118221258	cxcr3.2	c-X-C chemokine receptor type 3-like	f-agatttagtggctggcctgt; r-ctgcagctgccaatgttact
118226202	ncf2	Neutrophil cytosol factor 2	f-cctttgcactgtccttgcag; r-ccacacagccagaggactta
118217895	map3k4	mitogen-activated protein kinase 4, transcript variant X1	f-caccacctccttggtgact; r-agcttaagaacgaggccctt
118217281	LOC118217281	transmembrane protein 98-like	f-acgtctcctggatctcctct; r-tccctgggtagctggagt
118236408	fosl1b	FOS like 1, AP-1 transcription factor subunit b	f-aactacaccgccatccttca; r-tgacagaagaagcctgtcgt
118227292	LOC118227292	C-C motif chemokine 17-like	f-caccacctccttggtgact; r-agcttaagaacgaggccctt

2.8 Interaction network between DE-lncRNAs and Target DEGs

Location related target gene analysis was used by co-location (prediction of *cis* target gene according to the location relationship of lncRNA-mRNA, the range of screening is within 100k) and expression related target gene analysis was used by co-expression (number of samples = 9). Prediction of target gene was according to the expression correlation between DE-lncRNA ($p_{adj} < 0.05$) and mRNA when the correlation coefficient was greater than 0.95. To analyze the profiles of lncRNA-mRNA related DEGs interaction network and explore the potential roles of key lncRNAs in the infected eel pre versus post Freund's adjuvant inoculation, the correlation of co-location and co-expression analysis of DE-lncRNAs and mRNA related DEGs were used to analyze the anti-infection related lncRNAs. The Pearson correlation coefficient between lncRNA and mRNA greater than 0.99 was used as target DEGs ($p_{value} < 0.05$) for constructing network map of the lncRNA-mRNA interaction. Cytoscape software (version 3.5.1) was used to build co-location and co-expressed network between DE-lncRNAs and DEGs.

2.9 Statistical Analysis

Significant differences between two groups with the resulting *p* values of the DEGs and transcripts were adjusted to p_{adj} ($p_{adj} < 0.05$). Average data of bacterial plate colony count of each sample was transformed to $\log_{10}(\text{cfu}/\text{mg})$, and based on the differences of mean \pm SEM of the data, the origin 2017 software was used to map. Chi-square test was used to determine the differences in relative percent survival (RPS) post the *Ea* challenge between two infected groups of eels.

2.10 Data Accessibility

All transcriptome sequencing data have been uploaded to NCBI and the BioProject ID is PRJNA736610 (<https://www.ncbi.nlm.nih.gov/biosample/19655012-19655020>).

3. Results

3.1 The RPS, Bacterial Quantity and Pathological Changes

At 14 days post the challenge (dpc) of *Ea*, the mortality rates of eels in two groups were 86% and 43% corresponding to 50% RPS in FCIA_Li vs Con_Li (Fig. 1A). χ^2 test (Chi-Square) showed that there was significant difference ($p < 0.05$) in cumulative mortality between FCIA_Li and Con_Li group from 4 to 14 dpc. Average bacteria load of $10^{4.2}$ cfu and $10^{3.7}$ cfu per mg liver in the eels of Con_Li group, corresponding to average $10^{2.1}$ cfu and $10^{2.2}$ cfu that of FCIA_Li group at 24 and 48 h post challenge (hpc) (Fig. 1B). In the FCIA_Li group, slight edema of hepatocytes and blood coagulation in dilate hepatic vessels were observed at 48 hpc (Fig. 1C). In the liver of uninfected Li group, no colony was showed on the plate at 24 and 48 h sampling, and the hepatocytes were normal as well as red blood cells kept in the blood vessels at 48 h sampling (Fig. 1B, 1D). However, thrombi formed in the dilate hepatic vessels, celluloid degeneration of vascular wall and hepatocyte atrophy with eosinophilic cytoplasm in the Con_Li group were observed in the eels at 48 hpc (Fig. 1E).

3.2 Quality of RNA-seq

The quality evaluation of sequencing output data was shown in Table 2. Compared to the genome DNA of *A. anguilla*, the average sequencing base number of livers in two infection group was more than 14.5G, but only 9.6 G in the uninfected livers. The average total mapping of 9 samples was more than 81.8 according to the annotation file of *A. anguilla* (. gff). In all 9 samples, the base error rate of more than 94.35 fragments was less than 1% (Q20), and the base error rate of more than 87.97% fragments was less than 1‰ (Q30). Mapping rate of 9 samples between reads and genome of *A. anguilla* were showed in the Supplementary Table 1.

Table 2
RNA-seq quality of 9 samples in 3 groups

Sample name	total reads	total mapped	Clean reads	Clean bases(G)	Error rate (%)	Q20 (%)	Q30 (%)	GC content (%)
Con_Li1	101940598	90565121 (88.84%)	96420274	14.46G	0.03	96.87	91.87	51.06
Con_Li2	107148836	94341171 (88.05%)	91304806	13.7G	0.03	96.85	91.89	51.54
Con_Li3	106211632	91289281 (85.95%)	105554440	15.83G	0.03	96.59	91.44	50.92
Li_1	61897404	53895380 (87.07%)	61897404	9.28G	0.03	96.82	91.87	50.83
Li_2	64393862	52698760 (81.84%)	64393862	9.66G	0.03	94.35	87.97	50.77
Li_3	65662412	57950354 (88.25%)	65662412	9.85G	0.03	96.72	91.61	51.07
FCIA_Li1	93326318	83456782 (89.42%)	89180210	13.38G	0.03	97.04	92.14	50.44
FCIA_Li2	104415120	93775227 (89.81%)	104111930	15.62G	0.03	97.01	92.09	50.26
FCIA_Li3	104068460	89989477 (86.47%)	104893060	15.73G	0.03	96.85	91.84	50.24

3.3 Heat map clusters of differentially expressed genes and transcripts

From the comparison to the sequencing data of *A. anguilla* genome, the results of two-way cluster analysis showed quantity of DEGs and DE-mRNAs was about 10 times as the DE-lncRNAs and DE-TUCPs between 3 groups (Fig. 2). The results of DEGs and DE-mRNAs clustering showed the samples in the FCIA_Li group were similar to that of the Li group, but distinct differences were observed between these 6 samples and 3 samples in the Con_Li group (Fig. 2A, 2B). Simultaneously, the clustering results of DE-lncRNAs and DE-TUCPs (Fig. 2C, 2D) showed samples between 3 groups were different contrast to 3 samples in the lncRNAs were similar. Therefore, compared to the results of Gene, mRNA and TUCP clustering, the difference of the lncRNA between inter groups is much greater than that of intra groups.

3.4 DE-lncRNAs and the Target DEGs

In total of 9 samples, 13499 lncRNAs were expressed including 10176 annotated and 3423 novel lncRNAs (Supplementary Table 2). The Venn map showed 61, 63 and 76 DE-lncRNAs independently expressed in 3 comparisons of Con_Li vs Li, FCIA_Li vs Li and FCIA_Li vs Con_Li, corresponding to 22, 25 and 28 cross lncRNAs between the 3 comparisons (Fig. 3A), and in the volcano map, there were 44, 71 and 34 significantly upregulated corresponding to 67, 58 and 76 downregulated in the 3 comparisons (Fig. 3B). Compare to the

Con_Li group, 88 and 96 GO terms were significantly enriched ($qvalue < 0.05$) in co-expression (Supplementary Table 3) and co-location (Supplementary Table 4) DEGs targeted by 129 DE-lncRNAs in the FCIA_Li group. Top 50 enrichment GO terms of Co-expression showed 10 processes in BP, 4 processes in CC and the protein binding process in MF were distinctively enriched by more than 1000 regulated DEGs (Fig. 3C), and top 52 enrichment GO terms showed protein binding process in MF was distinctively enriched by 346 regulated DEGs in co-location (Fig. 3D). In the compare of FCIA_Li vs Con_Li, it was showed that 129 DE-lncRNAs targeted 7742 genes in co-expression (Supplementary Table 5), of which 8 KEGG pathways were significantly enriched (Fig. 3E) and the input vs background gene number were higher than 0.376. The co-location of 129 DE-lncRNAs target 942 genes in this compare (Supplementary Table 6), and the KEGG pathway of cell adhesion molecules (CAMs) was significantly enriched (Fig. 3F).

3.5 Validation of qRT-PCR for RNA_seq

In 23 verified DEGs, the fold change of 20 DEGs kept at the same level, but 2 DEGs (FOS like and serpin peptidase) were higher and the solute carrier family 7 was lower in RNA-seq contrast to the result of qPCR (Fig. 4). Compare to the Con_Li group, a lot of immune related genes were markedly upregulated in the FCIA_Li group, including complement component, lysozyme C, alpha-2-macroglobulin, H-2 class histocompatibility antigen, interferon regulatory factor, toll-like receptor, Neutrophil cytosol factor, mitogen-activated protein and C-C motif chemokine 17 (Fig. 4A, 4C). The linear fit of 23 genes expression showed correlative coefficient between the two methods was nearly 0.7 (Fig. 4B), and 17 genes were significantly unregulated as well as 4 genes were downregulated in the FCIA_Li group (Fig. 4C).

3.6 Interaction between DE-lncRNAs and Target DEGs

Interactions of lncRNAs and the target genes in the compare of FCIA_Li vs Con_Li showed 118 DE-lncRNAs ($padj < 0.05$) targeted 1161 DEGs and formed total of 8474 and 333 related links (degrees) in co-expression and co-location network (Fig. 5). Of which 16 DE-lncRNAs linked with 860 DEGs in the co-expression and 79 DEGs in the co-location were showed in Fig. 6 and Table 3. Two key interactions of an up (TCONS_00176927) and a downregulated (TCONS_00248653) lncRNAs directly targeted 291 (Fig. 6A) and 265 DEGs (Fig. 6B), and most of the degrees were co-expression except 6 co-location networks. Twelve lncRNAs target 81, 56, 39, 33, 26, 23, 25, 22, 21, 18, 14 and 14 DEGs in that order showed 6 lncRNAs (2 novel lncRNAs of XR_004763605.1 and XR_004764431.1, 4 annotated lncRNAs of TCONS_00356044, TCONS_00253920, TCONS_00073811 and TCONS_00094663) were downregulated, and 6 lncRNAs (TCONS_00411949, TCONS_00034988, TCONS_00034941, TCONS_00019338, TCONS_00086499, TCONS_00017692) were upregulated (from Fig. 6C to Fig. 6N). TCONS_00209209 and TCONS_00384582 target 5 and 6 DEGs respectively were upregulated (Fig. 6O, 6P).

Table 3
Significant fpkm difference of 16 DE-lncRNAs and the target gene degrees

lncRNA_ID	Figure 5	target gene degrees	FCIA_Li fpkm	Con_Li fpkm	log ₂ FC	pvalue	padj
TCONS_00176927	A	291	0.330	0.000	12.528	7.76E-05	1.2E-02
TCONS_00248653	B	265	0.267	0.000	-12.220	1.27E-04	1.7E-02
XR_004763605.1	C	81	0.002	1.980	-11.869	2.35E-04	2.5E-02
XR_004764431.1	D	56	0.279	711.041	-11.725	4.00E-06	1.5E-03
TCONS_00356044	E	39	0.010	5.080	-9.059	4.02E-04	3.5E-02
TCONS_00253920	F	33	0.002	7.857	-9.339	1.44E-04	1.8E-02
TCONS_00073811	G	26	1.370	29.274	-4.691	2.80E-04	2.9E-02
TCONS_00094663	H	23	0.000	7.761	-13.512	6.67E-04	4.9 E-02
TCONS_00411949	I	25	0.565	0.000	12.909	3.15E-5	6.5 E-03
TCONS_00034988	J	22	1.786	0.000	14.667	8.42E-08	6.25E-05
TCONS_00034941	K	21	0.711	0.000	14.543	1.81E-07	1.21E-04
TCONS_00019338	L	18	2.399	0.000	16.075	2.158E-04	2.4E-02
TCONS_00086499	M	14	0.503	0.000	12.861	6.98E-05	1.2E-02
TCONS_00017692	N	14	0.730	0.000	10.861	7.93E-06	2.6E-03
TCONS_00209209	O	6	152.1	0.000	19.233	1.13E-06	5.4E-04
TCONS_00384582	P	5	5.860	0.077	5.833	4.22E-04	3.6E-02
XR: novel lncRNA							

4. Discussion

In recent years, studies on the septicemia of cultivated fish caused by *Ea* have been reported (Armwood et al., 2019; Shao et al., 2015), but the molecular mechanism of the anti-infection in eel is not clear. In a previous study, we found that the *Ea* mainly invaded the liver of eels (Zhai et al., 2021), and in this study the infected liver was found thrombosis, celluloid degeneration of vascular wall and hepatocyte atrophy in the control infected eels (Fig. 1E). Eels in the FCIA_Li group showed slight pathological changes in the liver post the challenge of *Ea* (Fig. 1C), and the RPS of FCIA_Li vs Con_Li was 50% due to the liver bacteria load of FCIA_Li group was much lower than that of the Con_Li group at 24 and 48 hpc (Fig. 1B). Based on the RNA-seq of mRNA and lncRNA, the lncRNAs of European eels in the compare of FCIA_Li vs Con_Li were preliminarily explored, and the anti-infection related DEGs targeted by DE-lncRNAs ($p_{adj} < 0.05$) were firstly analyzed to reveal the anti-infection effect of the FCA and FIA adjuvant post the challenge of *Ea*.

lncRNA has been found to play an important role in the pathogenesis of many diseases (Chen et al., 2013). From the functional point of view, lncRNA mainly acts on the transcription, post transcription, translation and apparent level of the target gene respectively through *Cis* and *Trans* regulation to regulate the expression of the target gene (Florian and Joshua, 2018), so as to find out the different GO term or KEGG pathways of different treatments through the regulation of lncRNA (Schmittand and Chang, 2016). Co-location refers to the fact that lncRNA may regulate the nearby protein coding genes through analyzed the genes within 100 kb upstream and downstream of lncRNA (Bao et al., 2019). In this study, the co-expression and co-location of lncRNA and mRNA were used to predict the target genes of all DE-lncRNAs. The results showed that there were 129 DE-lncRNAs between 2 infection groups of eels, and the target DEGs in co-expression and co-location were as high as 7742 and 942, respectively.

In terms of the RNA-seq in eel liver, the average number of total reads of the Li group was 9.5 G while it was more than 14 G in two infection groups, indicating *Ea* infection promoted the gene transcription of the infected eels (Houtz et al., 2017). In this study, we also analyzed the DEGs, DE-mRNAs and DE-lncRNAs. The results showed no distinctive difference between Li and FCIA_Li groups in DEGs and DE-mRNAs, but DE-lncRNAs were distinctively different (Fig. 2) and it was selected to investigate the cause of lower mortality in the FCIA_Li group (Fig. 1A). So far, there is no report on the molecular mechanism of the protection effect of Freund's adjuvant, and this study will preliminarily reveal the nonspecific protective mechanism of the adjuvant.

European eels were inoculated with the FCA and FIA at 0 d and 14 d respectively to boost the protective effect to the *Ea* infection, and the results showed the RPS was 50% in European eels, much higher than 11% RPS after *Ea* challenge post 28 d of the solo FIA inoculated (He et al., 2020). Reason for RNA-seq at 48 hpc was that eels start to die from the third day in the FCIA group resulting in unavailable sampling (Fig. 1A), and significant bacteria quantity and obvious pathological changes between the eel livers in two infection groups were observed at 48 hpc (Fig. 1B-E). Venn and volcano map of DE-lncRNAs showed, compared to the Li group, most of the DE-lncRNAs in two infected groups were downregulated (Fig. 3B, 44 and 34 significantly upregulated corresponding to 67 and 76 downregulated). However, volcano map showed 71 upregulated and 58 downregulated lncRNAs in the compare of FCIA_Li vs Con_Li group. Therefore, the DE-lncRNAs between two infected groups more likely reveal the anti-infection molecular mechanism of the Freund's adjuvant to the *Ea* challenge (Huang et al., 2015).

The results showed that 88 and 96 GO terms were enriched ($p < 0.05$) in the co-expressing and co-location target genes respectively, including cellular response to stimulus, membrane, protein binding and binding processes et al (Fig. 3C, 3D). Of which the process of cellular response to stimulus was directly correlate with the immune function of the host (Liu et al., 2017). Eight enriched KEGG pathways were found in the co-expression DEGs targeted by lncRNAs (Fig. 3E), among which the pathways of neuroactive ligand-receptor interaction (Wang et al., 2013), Calcium signaling pathway and Wnt signaling pathway (De, 2011), MAPK signaling pathway (Wu et al., 2019), CAMs (Krishnan et al., 2019), and Cytokine-cytokine receptor interaction (Han et al., 2019) were directly related to non-specific immune clearance function.

Cell adhesion molecules (CAMs) are glycol-proteins expressed on the cell surface and play a critical role in a wide array of biologic processes that include hemostasis, the immune response, inflammation, embryogenesis, and development of neuronal tissue (Khodabandehlou et al., 2017). There are four main groups: the integrin family, the immunoglobulin superfamily, selectins, and cadherins (Samanta & Almo, 2015). Membrane proteins that mediate immune cell-cell interactions fall into different categories, namely those involved in antigen recognition, costimulation and cellular adhesion (Gennarini & Furley, 2017). There is only the CAMs KEGG pathway was enriched in co-location (Fig. 3F) in this study, and 15 DEGs in CAMs targeted by 6 DE-lncRNAs mainly encodes Myelin-associated glycoprotein (Bornhöfft et al., 2018), B-cell receptor CD22 (Li et al., 2019), Class I histocompatibility antigen (He et al., 2020) and Hemicentin proteins (Schultz et al., 2005). These proteins played important role in the process of the host anti-*Ea* infection.

In this study, 23 immune-related DEGs were randomly selected for qRT-PCR verification. Although 20 DEGs were basically kept at the same level, there were some differences between the results of qPCR verification and RNA-seq (Fig. 4) and the fit linear result showed their correlative coefficient is relatively low, which probably due to the multiple transcripts of some gene in eukaryotic cells. Primers used in qPCR is actually designed based on the level of transcripts, but RNA-seq can be used for differential analysis at both gene and transcripts level. For the same gene, qPCR is the difference in the expression level of a single transcript between samples, while RNA-seq is the comprehensive result of the expression level of multiple transcripts due to alternative splicing of a gene. Compare to the Con_Li group, 9 genes of 23 immune related genes increased more than 10 times in the FCIA_Li group (Fig. 4C), indicating these genes involved in nonspecific immunity in eels (Zhao et al., 2020; He et al., 2020; Xiao et al., 2022).

The interaction between DE-lncRNAs of 2 infection groups and the target DEGs through co-expression and co-location showed 129 DE-lncRNAs targeted 8684 DEGs. To compare the possible anti-bacterial function of the target DEGs, we selected 16 DE-lncRNAs changed more than 20 times between 2 infected groups (Fig. 5 & Fig. 6; Table 3). The result showed most of DEGs targeted by upregulated DE-lncRNAs in the FCIA_Li group were directly or indirectly involved in the immune function of the host, but that of DEGs targeted by upregulated DE-lncRNAs in the Con_Li group were closely related to immunosuppression or apoptosis. Some of the upregulated DEGs were also verified by the qRT-PCR method (Fig. 4). Therefore, the Freund's adjuvant enhanced the non-specific immune function of European eel and prevented the apoptosis of hepatocytes after bacterial infection, but immune function of eels in the control group was suppressed after the *Ea* infection and hepatocytes were apoptotic due to pro-inflammatory factors, which eventually led to the increased mortality of infected eels.

5. Conclusion

Compared to the eels inoculated by FCA and FIA, thrombus in the hepatic vessels, necrosis and atrophy of hepatocytes were observed, and a large number of bacteria were isolated from the control eels corresponding to 50% RPS in FCIA_Li vs Con_Li. The Strand-Specific RNA-seq showed obvious difference appeared in the clustering of DE-lncRNAs contrast to that of DEGs and DE-mRNAs. In total, 13499 lncRNAs were expressed in 9 samples with 10176 annotated and 3423 novel lncRNAs, of which 129 DE-lncRNAs were highlighted between two infected groups of FCIA_Li and Con_Li. One hundred and eighty-four enriched GO terms indicated DEGs targeted by 129 DE-lncRNAs in co-expression and co-location were mainly involved in single-organism cellular process, biological regulation, regulation of cellular process and response to stimulus in BP, component of membrane in CC and protein binding in MF. The target DEGs were enriched in Eight KEGG pathways in co-expression and enriched in cell adhesion molecules pathway in co-location. The interaction between 129 DE-lncRNAs and 8684 target genes in the compare of FCIA_Li vs Con_Li showed 118 DE-lncRNAs target 1161 DEGs and formed a total of 8474 and 333 related links in co-expression and co-location network, of which 16 crucial DE-lncRNAs linked with 860 DEGs in co-expression and 79 DEGs in co-location were further analyzed. The DE-lncRNAs revealed in our study will accelerate the understanding of the underlying *Edwardsiella* infection and fish anti-infection processes.

Declarations

Funding

This work was financially supported by Opening Foundation of Engineering Research Center of the Modern Industry Technology for Eel (RE202206).

Author statement

Under supervision by Songlin Guo, **Liqun Wu**: translation, editing, data curation. **Zhijie Yin**: inoculation, sampling, data curation. **Zheng Zhijin**: fish culture, sampling. **Yijun Tang**: editing. **Songlin Guo**: funding acquisition, formal analysis, methodology, project administration, resources, software, supervision, validation, writing original draft and editing.

Declaration of Competing Interest

The authors do not have financial and non-financial competing interests and the manuscript is approved by all authors for publication.

Ethics Statement

The fish used in this study were cultivated under protocols approved by the Jimei University Animal Care Committee (2011-59), and all experiments complied with the current laws of China and international organizations for the use of experimental animals.

References

1. Aciole Barbosa, D., Araújo, B.C., Branco, G.S. et al. 2022. Transcriptomic Profiling and Microsatellite Identification in Cobia (*Rachycentron canadum*), Using High-Throughput RNA Sequencing. *Mar Biotechnol* 24, 255–262.
2. Alessandra, B., Thomas, R., Gingeras, R.G., 2017. Comparative transcriptomics in human and mouse. *Nat. Rev. Genet.* 18(7), 425–440.
3. Armwood, A.R., Camus, A.C., López-Porrás, A., Ware, C., Griffin, M.J., Soto, E., 2019. Pathologic changes in cultured Nile tilapia (*Oreochromis niloticus*) associated with an outbreak of *Edwardsiella anguillarum*. *J. Fish. Dis.* 42 (10), 1463–1469.
4. Bao, Z., Yang, Z., Huang, Z., Zhou, Y., Cui, Q., Dong, D., 2019. LncRNADisease 2.0: An updated database of long non-coding RNA-associated diseases. *Nucleic Acids Res.* 47(D1), D1034–D1037.
5. Bornhöfft, K.F., Goldammer, T., Rebl, A., Galuska, S.P., 2018. Siglecs: A journey through the evolution of sialic acid-binding immunoglobulin-type lectins. *Dev. Comp. Immunol.* 86, 219–231.
6. Chen, G., Wang, Z., Wang, D., Qiu, C., Liu, M., Chen, X., Zhang, Q., Yan, G., Cui, Q., 2013. LncRNA Disease: a database for long-non-coding RNA-associated diseases. *Nucleic Acids Res.* (D1), D983-D986.
7. De, A., 2011. Wnt/Ca²⁺ signaling pathway: a brief overview. *Acta Biochim. Biophys. Sin.* 43(10), 745–56.
8. Duan, L., Feng, J., Lin, P., Guo, S., He, L., Xiao, Y., 2019. Evaluation of an outer membrane protein as a vaccine against *Edwardsiella anguillarum* in Japanese eels (*Anguilla japonica*). *Aquaculture.* 498, 143–150.
9. Florian, K., Joshua, T.M., 2018. Functional Classification and Experimental Dissection of Long Noncoding RNAs. *Cell.* 172(3), 393–407.
10. Gennarini G, Furley A. Cell adhesion molecules in neural development and disease. *Mol Cell Neurosci.* 2017; 81: 1–3.
11. Ghosh, S., Chan, C.K., 2016. Analysis of RNA-Seq Data Using TopHat and Cufflinks. *Methods Mol. Biol.* 1374, 339–361.
12. Guo, S., Feng, J., Xiong, J., et al., 2011. Immunohistochemical localization and pathological observation of *Aeromonas hydrophila* in European eel (*Anguilla anguilla*). *J. Huazhong Agric. Univ.* 30 (4), 494–499.
13. Guo, S., Hu, L., Feng, J., Lin, P., He, L., Yan, Q., 2019. Immunogenicity of a bivalent protein as a vaccine against *Edwardsiella anguillarum* and *Vibrio vulnificus* in Japanese eel (*Anguilla japonica*). *Microbiologyopen.* 8(6), e00766.
14. Guo, S.L., Wang, Y., Guan, R.Z., Feng, J.J., Lu, P.P., 2013. Immune effects of a bivalent expressed outer membrane protein to American eels (*Anguilla rostrata*). *Fish Shellfish Immunol.* 35(2), 213–220.
15. Han, C., Li, Q., Chen, Q., Zhou, G., Huang, J., Zhang, Y., 2019. Transcriptome analysis of the spleen provides insight into the immunoregulation of *Mastacembelus armatus* under *Aeromonas veronii* infection. *Fish Shellfish Immunol.* 88, 272–283.
16. Harrow, J., Frankish, A., Gonzalez, J.M., Tapanari, E., et al., 2012. GENCODE: the reference human genome annotation for The ENCODE Project. *Genome Res.* 22(9), 1760–1774.
17. He, L., Wu, L., Lin, P., Zhai, S., Guo, S., Xiao, Y., Wan, Q., 2020. First expression and immunogenicity study of a novel trivalent outer membrane protein (OmpII-U-A) from *Aeromonas hydrophila*, *Vibrio vulnificus*

- and *Edwardsiella anguillarum*. Aquaculture. 519, 734932
18. He, L., Wu, L., Tang, Y., Lin, P., Zhai, S., Xiao, Y., 2020. Immunization of a novel outer membrane protein from *Aeromonas hydrophila* simultaneously resisting *A. hydrophila* and *Edwardsiella anguillarum* infection in European eels (*Anguilla anguilla*). Fish Shellfish Immunol. 97(2), 300–312.
 19. He W, Wu L, Li S, Guo S. Transcriptome RNA-seq revealed lncRNAs activated by *Edwardsiella anguillarum* post the immunization of OmpA protecting European eel (*Anguilla anguilla*) from being infected. Fish Shellfish Immunol. 2021; 118: 51–65.
 20. Houtz, P., Bonfini, A., Liu, X., Revah, J., Guillou, A., Poidevin, M., Hens, K., Huang, H.Y., Deplancke, B., Tsai, Y.C., Buchon, N., 2017. Hippo, TGF- β , and Src-MAPK pathways regulate transcription of the upd3 cytokine in Drosophila enterocytes upon bacterial infection. PLoS Genet. 13(11), e1007091.
 21. Huang, L., Damle, S.S., Booten, S., Singh, P., Sabripour, M., Hsu, J., Jo, M., Katz, M., Watt, A., Hart, C.E., Freier, S.M., Monia, B.P., Guo, S., 2015. Partial Hepatectomy Induced Long Noncoding RNA Inhibits Hepatocyte Proliferation during Liver Regeneration. PLoS One. 10(7), e0132798.
 22. Jiao XD, Cheng S, Hu YH, Sun L. Comparative study of the effects of aluminum adjuvants and Freund's incomplete adjuvant on the immune response to an *Edwardsiella tarda* major antigen. Vaccine. 2010; 28(7):1832–1837.
 23. Khodabandehlou K, Masehi-Lano JJ, Poon C, Wang J, Chung EJ. Targeting cell adhesion molecules with nanoparticles using *in vivo* and flow-based *in vitro* models of atherosclerosis. Exp Biol Med (Maywood). 2017; 242(8): 799–812.
 24. Krishnan, R., Qadiri, S.S.N., Oh, M.J., 2019. Functional characterization of seven-band grouper immunoglobulin like cell adhesion molecule, Nectin4 as a cellular receptor for nervous necrosis virus. Fish Shellfish Immunol. 93, 720–725.
 25. Kumar, G., Rathore, G., Sengupta, U., Singh, V., Kapoor, D., Lakra, W.S., 2007. Isolation and Characterization of Outer Membrane Proteins of *Edwardsiella tarda* and Its Application in Immunoassays. Aquaculture. 272(1), 98–104.
 26. Li, Y.Q., Sun, L., Li, J., 2019. Macropinocytosis-dependent endocytosis of Japanese flounder IgM + B cells and its regulation by CD22. Fish Shellfish Immunol. 84, 138–147.
 27. Liu, Y., Xin, Z.Z., Zhang, D.Z., Wang, Z.F., Zhu, X.Y., Tang, B.P., Jiang, S.H., Zhang, H.B., Zhou, C.L., Chai, X.Y., Liu, Q.N., 2017. Transcriptome analysis of yellow catfish (*Pelteobagrus fulvidraco*) liver challenged with polyriboinosinic polyribocytidylic acid (poly I:C). Fish Shellfish Immunol. 68, 395–403.
 28. Olivier G, Evelyn TP, Lallier R. Immunity to *Aeromonas salmonicida* in coho salmon (*Oncorhynchus kisutch*) induced by modified Freund's complete adjuvant: its non-specific nature and the probable role of macrophages in the phenomenon. Dev Comp Immunol. 1985; 9(3): 419–32.
 29. Pertea, M., Pertea, G.M., Antonescu, C.M., Chang, T.C., Mendell, J.T., Salzberg, S.L., 2015. StringTie enables improved reconstruction of a transcriptome from RNA-seq reads. Nat. Biotechnol. 33(3), 290–295.
 30. Ramos-Espinoza FC, Cueva-Quiroz VA, Yunis-Aguinaga J, Alvarez-Rubio NC, Paganoti de Mello N, Engrácia de Moraes JR. Efficacy of two adjuvants administrated with a novel hydrogen peroxide-

- inactivated vaccine against *Streptococcus agalactiae* in Nile tilapia fingerlings. *Fish Shellfish Immunol.* 2020; 105: 350–358.
31. Reichley, S.R., Ware, C., Steadman, J., Gaunt, P.S., García, J.C., LaFrentz, B.R., Thachil, A., Waldbieser, G.C., Stine, C.B., Buján, N., Arias, C.R., Loch, T., Welch, T.J., Cipriano, R.C., Greenway, T.E., Khoo, L.H., Wise, D.J., Lawrence, M.L., Griffin, M.J., 2017. Comparative Phenotypic and Genotypic Analysis of *Edwardsiella* Isolates from Different Hosts and Geographic Origins, with Emphasis on Isolates Formerly Classified as *E. tarda*, and Evaluation of Diagnostic Methods. *J. Clin. Microbiol.* 55(12), 3466–3491.
 32. Robinson, E.K., Covarrubias, S., Carpenter, S., 2020. The how and why of lncRNA function: An innate immune perspective. *BBA-GENE REGUL MECH.* 1863(4), 194419.
 33. Samanta D, Almo SC. Nectin family of cell-adhesion molecules: structural and molecular aspects of function and specificity. *Cell Mol Life Sci.* 2015; 72(4):645–58.
 34. Schmittand, A.M., Chang, H.Y., 2016. Long Noncoding RNAs in Cancer Pathways. *Cancer Cell.* 29(4), 452–463.
 35. Schultz, D.W., Weleber, R.G., Lawrence, G., Barral, S., Majewski, J., Acott, T.S., Klein, M.L., 2005. HEMICENTIN-1 (FIBULIN-6) and the 1q31 AMD locus in the context of complex disease: review and perspective. *Ophthalmic Genet.* 26(2), 101–5.
 36. Shao, S., Lai, Q., Liu, Q., Wu, H., Xiao, J., Shao, Z., Wang, Q., Zhang, Y., 2015. Phylogenomics characterization of a highly virulent *Edwardsiella* strain ET080813T encoding two distinct T3SS and three T6SS gene clusters: propose a novel species as *Edwardsiella anguillarum* sp. nov. *Syst. Appl. Microbiol.* 38(1), 36–47.
 37. Tang, X., Zhan, W., Sheng, X., Chi, H., 2010. Immune Response of Japanese Flounder *Paralichthys olivaceus* to Outer Membrane Protein of *Edwardsiella tarda*. *Fish Shellfish Immunol.* 28(2), 333–343.
 38. Varet, H., Brillet-Guéguen, L., Coppée, J.Y., Dillies, M.A., 2016. SARTools: A DESeq2- and EdgeR-Based R Pipeline for Comprehensive Differential Analysis of RNA-Seq Data. *Plos One.* 11(6), e0157022.
 39. Valenzuela-Muñoz, V., Váldez, J.A. & Gallardo-Escárate, C. 2021. Transcriptome Profiling of Long Non-coding RNAs During the Atlantic Salmon Smoltification Process. *Mar Biotechnol* 23, 308–320.
 40. Wang, J., Yue, B., Zhang, X., Guo, X., Sun, Z., Niu, R., 2021. Effect of exercise on microglial activation and transcriptome of hippocampus in fluorosis mice. *Sci. Total Environ.* 760, 143376.
 41. Wu, X.M., Cao, L., Hu, Y.W., Chang, M.X., 2019. Transcriptomic characterization of adult zebrafish infected with *Streptococcus agalactiae*. *Fish Shellfish Immunol.* 94, 355–372.
 42. Xiao, Y., Wu, L., Guo, S., 2021. First identification of B-cell linear epitopes of outer membrane protein A (OmpA) of *Edwardsiella anguillarum* in rabbit and European eels (*Anguilla anguilla*). *Aquaculture.* 533(3), 736092.
 43. Xiao Y, Wu L, He L, Tang Y, Guo S, Zhai S. 2022. Transcriptomic analysis using dual RNA sequencing revealed a Pathogen-Host interaction after *Edwardsiella anguillarum* infection in European eel (*Anguilla anguilla*). *Fish Shellfish Immunol.* 120, 745–757.
 44. Xiu, Y., Li, Y., Liu, X., Su, L., Zhou, S., Li, C., 2021. Identification and Characterization of Long Non-coding RNAs in the Intestine of Olive Flounder (*Paralichthys olivaceus*) During *Edwardsiella tarda* Infection. *Front. Immunol.* 12, 623764.

45. Young, M.D., Wakefield, M.J., Smyth, G.K., Oshlack, A., 2010. Gene ontology analysis for RNA-seq: accounting for selection bias. *Genome Biol.* 11(2), 1–12.
46. Yousefi, H., Maheronnaghsh, M., Molaei, F., Mashouri, L., Reza, A.A., Momeny, M., Alahari, S.K., 2020. Long noncoding RNAs and exosomal lncRNAs: classification, and mechanisms in breast cancer metastasis and drug resistance. *Oncogene.* 39(5): 953–974.
47. Zhai, S., Xiao, Y., Tang, Y., Wan, Q., Guo, S., 2021. Transcriptome of *Edwardsiella anguillarum in vivo* and *in vitro* revealed two-component system, ABC transporter and flagellar assembly are three pathways pathogenic to European eel (*Anguilla anguilla*). *Microb. Pathog.* 104801.
48. Zhang, L., Ni, C., Xu, W., Dai, T., Yang, D., Wang, Q., Zhang, Y., Liu, Q., 2016. Intramacrophage Infection Reinforces the Virulence of *Edwardsiella tarda*. *J. Bacteriol.* 198(10), 1534–42.
49. Zhao J, Wu L, Zhai S, Lin P, Guo S. 2020. Construction expression and immunogenicity of a novel trivalent outer membrane protein (OmpU-A-II) from three bacterial pathogens in Japanese eels (*Anguilla japonica*). *J Fish Dis.* 43(5):519–529.
50. Zhao, N., Jia, L., Li, G. et al. Comparative Mucous miRomics in *Cynoglossus semilaevis* Related to *Vibrio harveyi* Caused Infection. *Mar Biotechnol* 23, 766–776 (2021).

Figures

Figure 1

The cumulative mortality rate of eels challenged by *Ea* B79 (A), Bacteria load in the liver (\log_{10} cfu/mg) (B) and H.E staining results of liver sections of eels in FCIA_Li (C), Li (D) and Con_Li (E) group. A: cumulative mortality rate of eels challenged by *Ea* B79 in the Li and FCIA groups; * $p < 0.05$ between the FCIA_Li and the Con_Li group in 14 dpc. B: colony quantity per mg liver tissue of 2 challenged groups and colony growth of representative coating plates of 3 groups. * $p < 0.05$ and ** $p < 0.01$ between the FCIA_Li and the Con_Li group. C: slight atrophy of hepatocytes and blood coagulation in the hepatic vessels of eels infected by *Ea* after FCIA injection. D: normal hepatocytes and red blood cells in normal blood vessels of uninfected eels; E: hepatic vein dilation, thrombosis, atrophy and degeneration of hepatocytes, and necrosis of some hepatocytes of eels infected by *Ea*. Scale bar: 50 μ m

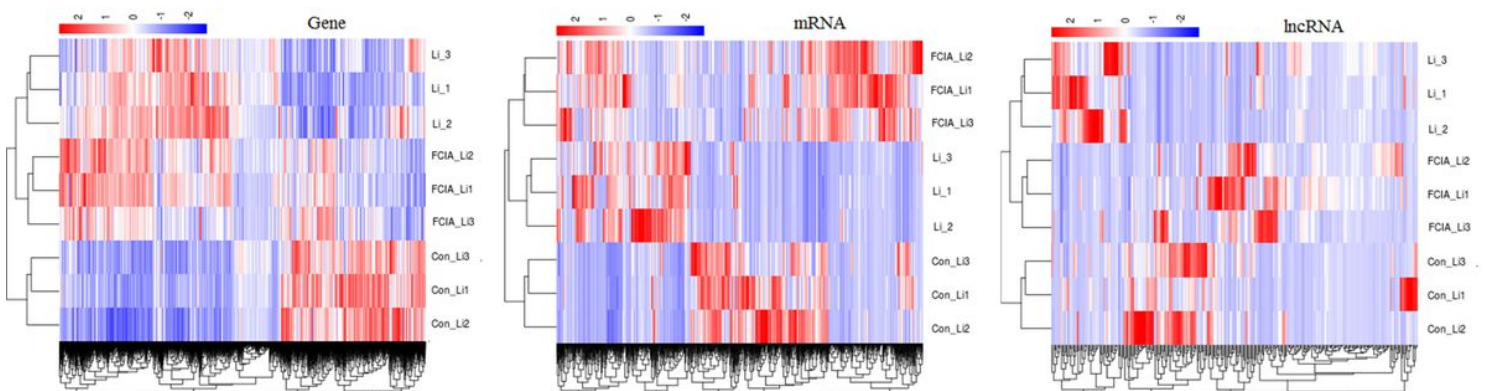


Figure 2

Heat map cluster of Genes (A) and transcripts of mRNA (B) and lncRNA (C) in 9 livers of 3 groups. Log₁₀ (fpmk+1) was transformed and clustered by hierarchical clustering method, and the results were expressed by Heat map.

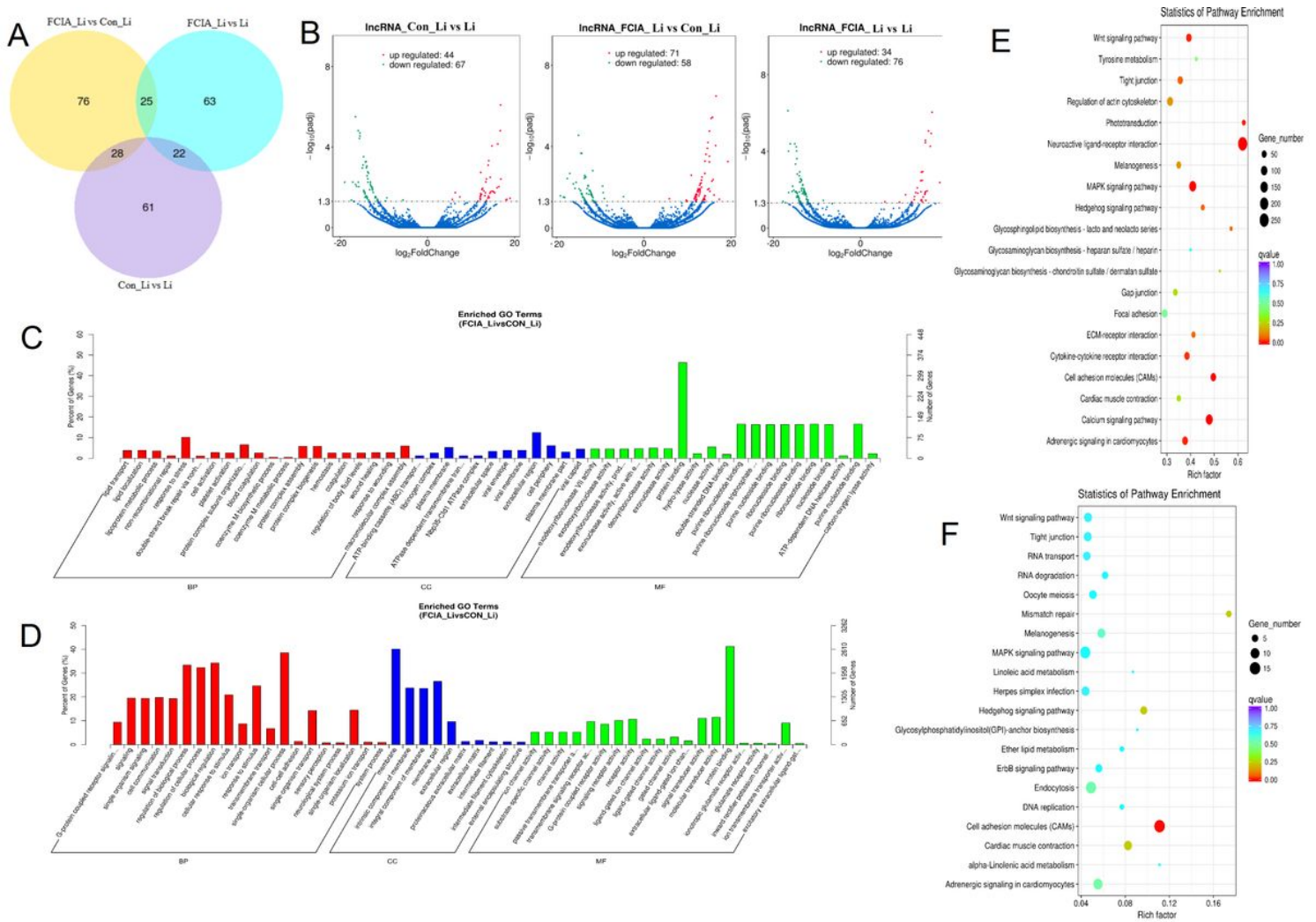
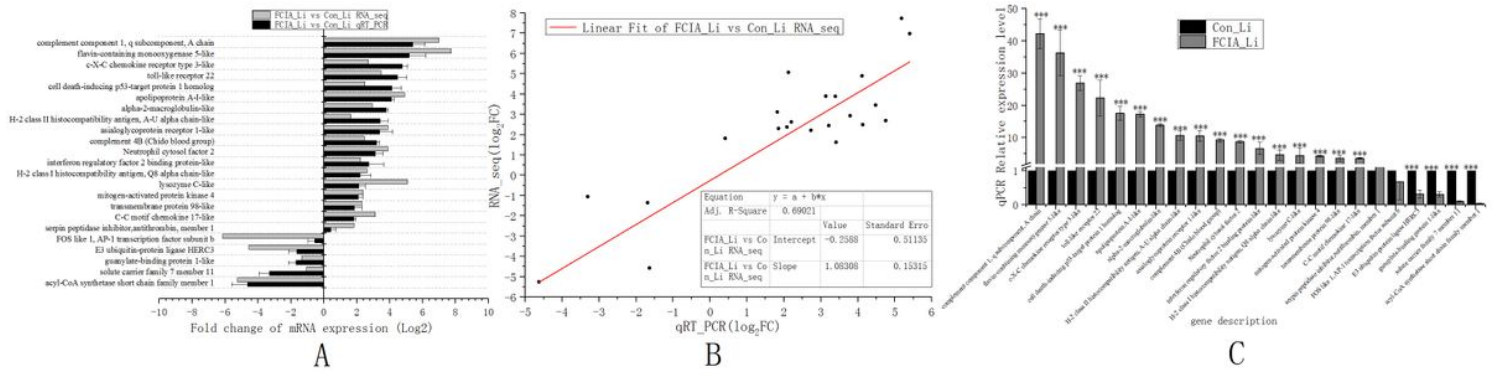


Figure 3

Venn (A) and volcano (B) map of DE-lncRNAs between 3 comparisons in 3 groups, the enrichment GO terms of significant up and down DEGs targeted by 158 DE-lncRNAs in co-expression (C) and co-location (D) in FCIA_Li vs Con_Li, and top 20 most enriched KEGG pathway of DEGs targeted by DE-lncRNAs in co-expression (E) and co-location (F) in FCIA_Li vs Con_Li. C&D: The ordinate is the corrected GO term enriched, and the abscissa is the ratio and number of DEGs in the term. BP: Biological process; CC: Cell Component; MF: Molecular Function. E & F: The vertical axis represents the KEGG enrichment analysis pathway, and the horizontal axis represents the rich factor ratio of the up or downregulated genes in the pathway. The size of the dots indicates the number of DEGs in the pathway, and the color of the dots corresponds to different q value ranges.



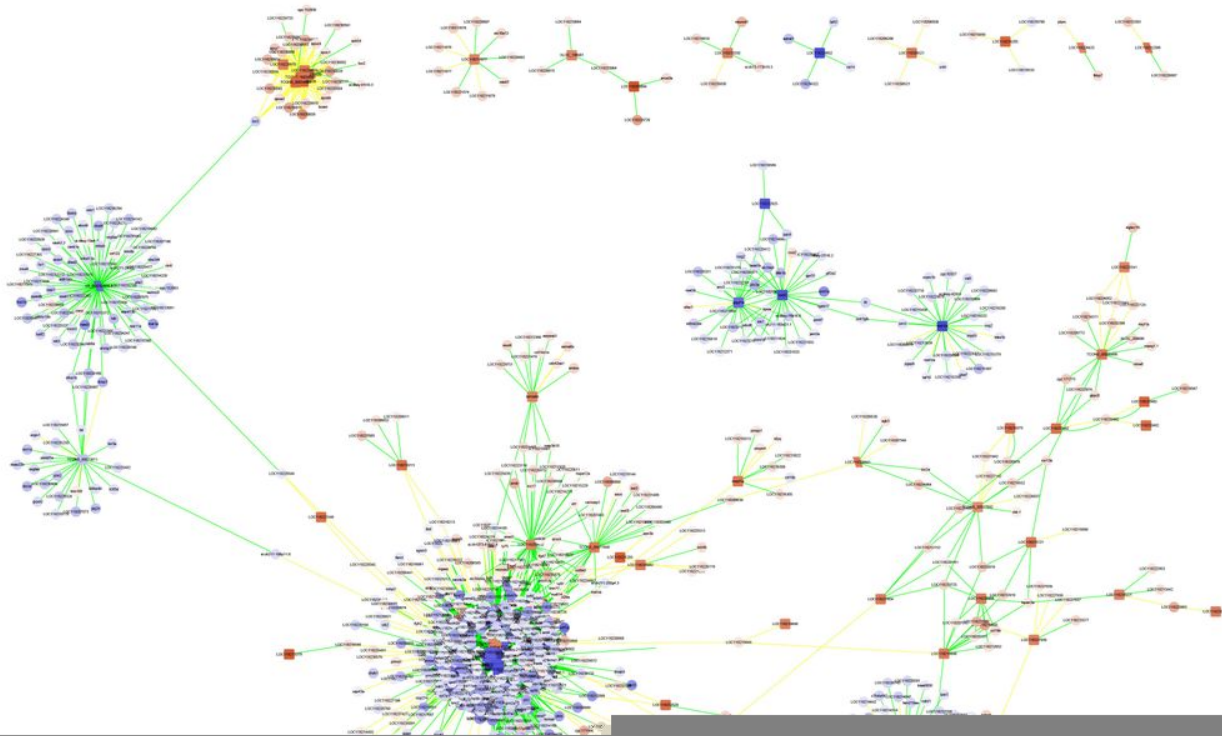


Figure 5

Gene expression network of the 118 DE-lncRNAs and 1161 DEGs. DE-lncRNAs and novel DE-lncRNAs are showed as rectangle and parallelogram shape as well as the target DE-mRNAs and novel DE-mRNAs are showed as ellipse and octagon shape. Red background indicates significant up-regulation and blue background indicates significant down-regulation; shade of the color indicates the degree of down and up regulations ($\log_2FC = -20$ to 20). The yellow and green edges that connect the nodes (lncRNAs and DEGs) represent co-location and co-expression relationship ($R > 0.99$ or $R < -0.99$).

Figure 6

Significant regulated lncRNA ($p_{adj} < 0.05$) target significant mRNA-related genes by co-expression (green line) and co-location (yellow line) in the compare of FCIA_Li vs Con_Li. Those that begin with the letter "TCONS" and "XR" represent the lncRNA, while those that begin with other number/letters represents target genes. Red background indicates significant up-regulation and blue background indicates significant down-regulation; shade of the color indicates the degree of down and up regulations ($\log_2FC = -20$ to 20). The yellow and green edges that connect the nodes (lncRNAs and DEGs) represent co-location and co-expression relationship.

Supplementary Files

This is a list of supplementary files associated with this preprint. Click to download.

- [SupplementaryTab.1Listofmappingrateof9samplesbetweenreadsandreferencedgenomeofA.anguilla.xlsx](#)
- [SupplementaryTab.2lncRNAfpkm.xlsx](#)
- [SupplementaryTab.3lncRNAGOexpressionall.xlsx](#)
- [SupplementaryTab.4lncRNAGOlocationall.xlsx](#)
- [SupplementaryTab.5DElncRNAtargetcoexpression.xlsx](#)
- [SupplementaryTab.6DElncRNAtargetcolocation.xlsx](#)